Published in final edited form as:
Biomaterials. 2012 February ; 33(6): 1821–1826. doi:10.1016/j.biomaterials.2011.11.015.

Plasmonic nanobubble-enhanced endosomal escape processes for selective and guided intracellular delivery of chemotherapy to drug-resistant cancer cells

Ekaterina Y. Lukianova-Hleb[a], **Andrey Belyanin**[a], **Shruti Kashinath**[a], **Xiangwei Wu**[b], and **Dmitri O. Lapotko**[a,c,*]

[a]Department of Biochemistry and Cell Biology, Rice University, Houston, 77005 TX, USA

[b]Department of Head and Neck Surgery, The University of Texas MD Anderson Cancer Center, Houston, 77030 TX, USA

[c]Department of Physics and Astronomy, Rice University, Houston, 77005 TX, USA

Abstract

Cancer chemotherapies suffer from multi drug resistance, high non-specific toxicity and heterogeneity of tumors. We report a method of plasmonic nanobubble-enhanced endosomal escape (PNBEE) for the selective, fast and guided intracellular delivery of drugs through a self-assembly by cancer cells of separately targeted gold nanoparticles and encapsulated drug (Doxil). The co-localized with Doxil plasmonic nanobubbles optically generated in cancer cells released the drug into the cytoplasm thus increasing the therapeutic efficacy against these drug-resistant cells by 31-fold, reducing drug dose by 20-fold, the treatment time by 3-fold and the non-specific toxicity by 10-fold compared to standard treatment. Thus the PNBEE mechanism provided selective, safe and efficient intracellular drug delivery in heterogeneous environment opening new opportunities for drug therapies.

Keywords

Liposome; Gold; Nanoparticle; Laser; Drug release; Drug delivery

1. Introduction

The precise intracellular delivery of drugs and other therapeutic and diagnostic agents to specific target cells is one of the ultimate goals of medicine and biology. Nanoparticles (NP) have successfully been used to carry drug [1–7], and to induce its release from other carriers [8–13] but the selectivity of NP targeting is limited by the unavoidable non-specific coupling of NPs to non-specific cells and consequent non-specific toxicity in heterogeneous cell systems such as tissues and tumors. The encapsulation of toxic drugs may reduce their non-specific toxicity [14,15], but at the same time limits drug release because of the lack of efficient release mechanisms. Diffusion-based and biologically-activated release mechanisms are slow, cannot be precisely controlled on-demand and do not augment the selectivity of drug delivery. Drugs may also be delivered following opto-, sono- and electro-poration of the cellular membrane [16–20], but these physical methods cannot discriminate

*Corresponding author. Rice University, Department of Biochemistry and Cell Biology, MS 140, 6100 Main Street, Houston, TX 77005, USA. Tel.: +1 713 348 3708; fax: +1 713 348 5154. dl5@rice.edu (D.O. Lapotko).

between target and bystander cells in a heterogeneous system and also cause non-specific toxicity. Thus, unless each target cell is first isolated [21–23], the rapid selective intracellular delivery of the drug into target cells in heterogeneous systems is not yet feasible, and this lack of a fast, selective and efficient means of effecting intracellular chemotherapy remains a principal challenge for medical practice.

Our approach to overcoming the above limitations is based on the unique properties of plasmonic gold NPs for targeting and remote optical activation. We recently developed a new class of nano-agents which are not NPs but transient events, vapor nano-bubbles, generated on-demand with short laser pulses around cell-specific clusters of plasmonic NPs, named plasmonic nanobubbles (PNBs) [24,25]. Cellular applications of PNBs use their mechanical, non-thermal, tunable and localized action that provides highly sensitive imaging and the guided elimination of target cells [26,27]. In particular, we discovered that the threshold energy of the laser pulse required to generate a PNB rapidly decreases with the size of the NP cluster [24–26]. This allows for the selective generation of PNBs at minimal optical energies and around the largest clusters of NPs selectively formed in target cells, while preventing the generation of PNBs around smaller clusters and single NPs in non-specific cells under the same optical energy [26,28,29]. Using the localized mechanical effect of PNBs we demonstrated the fast and efficient release of molecular cargo from individual liposomes [30] and the cell-specific and non-invasive gene transfection [28], as well as showing the potential of PNBs to guide their mechanical effect optically and acoustically.

Based on our developments, we hypothesized that target cell-specific intracellular delivery of drugs can be realized in a safe and rapid simultaneous treatment of heterogeneous cell systems with small PNBs, providing the selective formation in target cells of the mixed nanoclusters of gold NPs and drug capsules. We further hypothesized that target cells will self-assemble such mixed nanoclusters through, for example, the mechanism of receptor-mediated endocytosis (Fig. 1a). PNBs generated around gold NPs will disrupt co-localized capsules and the endosome membrane and will eject the drug into the cytoplasm within nanoseconds (Fig. 1e). To selectively form such nanoclusters, the cells will be separately treated with gold NPs and encapsulated drugs conjugated with target cell-specific vectors. Only target cells will accumulate a sufficient amount of gold NPs and of the encapsulated drug and thus will assemble the mixed nanoclusters (Fig. 1a), while unavoidable non-specific coupling of some drug capsules or NPs to normal cells will not form such nanoclusters (Fig. 1b) and thus will not be able to generate disruptive PNBs and the drug will not be released (Fig. 1f). Therefore, the selective self-assembly of an NP-drug nanocluster and its activation with a laser pulse for colocalized PNB generation will provide intracellular drug delivery with a single cell selectivity, while the extracellular drug can be totally removed after targeting and prior to the PNB generation. This universal mechanism should provide both high therapeutic efficacy and low non-specific toxicity of chemotherapy, because the localized nature of PNBs will release the drug only within individual target cells. This release will be done as a fast ejection, not slow diffusion and thus will provide high local concentration of the released drug. The optical and acoustical properties of PNBs will be used for real-time guidance of the drug release. We termed this mechanism plasmonic nanobubble-enhanced endosomal escape (PNBEE) and explored it *in vitro* in a heterogeneous mixture of normal and drug-resistant cancer cells.

2. Methods and materials

2.1. Cell model

We used multi drug-resistant HN31 squamous carcinoma cells (associated with head and neck cancers) expressing epidermal growth factor receptor (EGFR) and immortalized

normal human oral kerotinocyte NOM 9 cells. The NOM 9 cells were cultured in KGM Complete Medium (Cat# CC-3001) from Lonza in a 37°, 5% CO_2 incubator. The malignant cells were transfected with green fluorescent protein (GFP) to allow identification. The HN31 GFP stable cell line was built by transfecting the EGFP C1 plasmid into HN31 cells. The selecting marker was G418. The transfected cells were cultured in DMEM High Glucose medium (Cat# 10013 CV) from Mediatech supplemented with MEM Vitamin Solution (Cat# 11120) and MEM NEAA (Cat#11140) both from Gibco and penicillin-streptomycin (Cat# 30002 CT) from Mediatech in the same incubator. For co-culture, the cells were resuspended in KGM media and counted after trypsinization and neutralization. NOM 9 was mixed with HN31 GFP cell in 100:1 ratio and seeded at a density of 700,000 cells/ml in 15-well chambered slide (μ-Slide Angiogenesis, Ibidi LLC, Martinsried, Germany). Cell death was measured with Trypan Blue exclusion test in 72 h after the treatment by PNBs or drugs (Doxil liposomes or Doxorubicin).

2.2. Gold nanoparticles, Doxil conjugates and their targeting

50 nm hollow gold nanoshells (NS) were synthesized by galvanic replacement of gold on a silver core according to Zasadzinski et al. [8,31]. The advantages of this type of NP include low toxicity, reliable conjugation properties, relatively high photothermal efficiency and maximal PNB generation efficacy in the biologically safe near-infrared spectral region with reducing the PNB generation threshold laser fluence [24] down to a biologically safe level [32] 5–7 mJ/cm^2. NSs were characterized by optical spectroscopy and transmission electron microscopy. Maximal optical absorbance of NPs was 820 nm, in the near-infrared (NIR) window; NIR light is minimally absorbed by all endogenous molecules and by water. For active targeting and endocytosis, the NSs were covalently conjugated to Panitumumab antibody (directed to EGFR, over-expressed by HN31) by BioAssayWorks LLC (Ijamsville, MD). We used stock encapsulated anti-tumor drug, Doxil (Doxorubicin encapsulated into 85 nm liposomes). The Doxil liposomes (Ben Venue Laboratories, Inc, Bedford, OH) were also conjugated with the same antibody (Panitumumab) as described in [33–35] for their active targeting and endocytosis by cancer cells. Conjugated gold NSs (2.4×10^{10} particles/ml) and Doxil liposomes (5 μg/ml) were separately administered *in vitro* by incubating for 24 h with a co-culture of HN31/NOM9 cells under physiological conditions (37 °C). After that uncoupled NPs and liposomes were washed off prior to the generation of PNBs. Small size of NSs and of liposomes provided efficient targeting through receptor-mediated endocytosis of both components. As a result of such targeting NSs and Doxil liposomes were selectively internalized by target cells and formed mixed intracellular clusters [27,29,36–38], likely within endosomes. Uptake of NPs and Doxil by living cells was assayed with a confocal microscopy (LSM-710, Carl Zeiss MicroImaging GmbH, Germany) in the bright field, optical scattering (for imaging NSs) and two fluorescent (for a separate imaging GFP (at 520 nm) and Doxil (at 605 nm)) modes. Cancer cells were identified among normal cells in a co-culture through their green GFP-specific fluorescence. Therapeutic effect of PNBs and drug was measured in 72 h after the treatment with Trypan Blue exclusion test.

2.3. Generation and detection of plasmonic nanobubbles

PNBs were generated due to transient heating of gold NSs with single laser pulses to the temperatures well above the evaporation threshold for the NS environment. Single pump laser pulse (70 ps, 820 nm, PL-2250, Ekspla, Vilnius, Lithuania) was applied to cover simultaneously area with hundreds of cells. The laser fluence (in the range 15–40 mJ/cm^2) was experimentally determined at the level that provided almost 100% probability of the PNB generation in cancer cells with NS clusters and at the same time was below the PNB generation thresholds for small NS clusters and for individual NS. Laser beam diameter was 260 μm, and the cell sample was scanned by laser pulses at specific and variable fluence. The fluence of each laser pulse was measured by registering its image and measuring the

beam diameter at the sample plane with the imaging device (Luka, Andor Technology, Northern Ireland) and by measuring the pulse energy with the pulse energy meter (Ophir Optronics, Ltd., Israel). This scheme provided direct and precise measurements of the incident optical fluence at the cell plane for each excitation pulse. We used previously developed methods and experimental set-up [26] to image, detect and quantify the thermal and mechanical impacts of PNBs in individual cells through their optical scattering images and time-responses detected in parallel with two probe lasers. The shape of the time-response signal was specific and different for a heating-cooling effect without generation of PNB and for generation of PNB, while the duration of the PNB-specific response characterized the PNB lifetime. The maximal diameter of the PNB (which determines the therapeutic effect) is proportional to the PNB lifetime [24,25,39–41]. In addition, excellent optical scattering properties of the PNB [24] were used for its imaging in cells with the second, pulsed probe beam (576 nm, 70 ps, 0.1 mJ/cm^2). This beam was directed at the sample under high angle of incidence and with 10 ns delay relative to the excitation laser pulse. Thus only the light scattered by transient PNB was collected by microscope objective (20×) and detected by the mentioned above imaging devise. Operation of the all hardware was controlled by PC through the custom software modules developed with LabView platform.

3. Results and discussion

3.1. Plasmonic nanobubble-enhanced endosomal escape

Multi drug-resistant HN31 squamous cell carcinoma (associated with head and neck cancers) co-cultured with normal epithelial NOM9 cells were treated with the standard anti-cancer drug, Doxorubicin, in its liposome-encapsulated form, gold NS conjugates and PNBs. For active targeting and endocytosis, the Doxil and NSs conjugates were separately targeted at specific concentrations to the co-culture for 24 h and were then washed off prior to the generation of PNBs. Thus the cells were exposed only to the internalized drug and the exposure time was reduced to 24 h (clinical administration of Doxil assumes a 4–7 day exposure to the drug [42]). The efficacy and selectivity of NS clustering and colocalization with Doxil was analyzed with confocal microscopy (LSM-710, Carl Zeiss MicroImaging GmbH, Germany) in scattering (for NSs) and fluorescent (for Doxil) modes. Cancer cells showed NS clusters that were co-localized and mixed with clusters of Doxil (Fig. 1c and insert). Doxorubicin-specific red fluorescence was significantly suppressed in liposomes due to quenching effect. Intact HN31 cells and Doxil- and NS-treated normal cells (Fig. 1d and insert) did not show the fluorescent patterns shown in Fig. 1c and therefore we interpreted localized red images in Fig. 1c as the clusters of Doxil. As a rule they were co-localized with the images of NS clusters (blue in Fig. 1c and insert) and thus we concluded that the cancer cells selectively formed the mixed NS-Doxil clusters.

PNBs were generated by scanning the whole co-culture sample with single laser pulses (70 ps, 820 nm, PL-2250, Ekspla, Vilnius, Lithuania) at specific and variable fluence that was reduced below the level of PNB generation around single NSs but was sufficient to generate the PNBs around the largest intracellular clusters of NSs. PNBs were detected in individual cells with time-resolved optical scattering imaging (Fig. 1g, h), while their maximal size was measured as their lifetime (that correlates to PNB size [22,32]) through the duration of optical scattering time-responses of the PNBs (Fig. 1j). PNB images and responses showed a high selectivity of PNB generation in cancer cells (Fig. 1g, j) while the normal cells produced no or small PNBs under identical NSs and laser treatment (Fig. 1h, j). PNBs were generated when the fluence of the laser pulse exceeded a specific threshold for NS cluster (vertical dashed line in Fig. 1i), and above that threshold their maximal size (lifetime) was tuned through the fluence of the laser pulse. High selectivity of PNB generation in cancer cells was observed in the whole range of applied laser fluences (Fig. 1i). This result also

indicated a good tunability of the PNB size with the fluence of the excitation laser pulse. A comparison of images of PNBs (Fig. 1g) and nanoclusters (Fig. 1c) showed that, as a rule, PNBs were co-localized with the largest mixed nanoclusters of NS (sources of PNBs) and Doxil liposomes in cancer cells, while none of those was observed in normal cells (Fig. 1d,h).

The levels of cell death were measured 72 h after the PNB treatment of the co-culture of cancer and normal cells. Cancer cells were identified through the green fluorescence of GFP (Fig. 2a) and the dead cells were identified through their blue color after staining with Trypan Blue (Fig. 2b). Direct exposure to Doxil without PNB treatment had a limited effect on malignant cells and even higher toxicity to normal cells and required high doses of drug to achieve cell death (Fig. 2c). Parallel PNB treatment of the same cells without Doxil showed the increase of the cell death level with the size (lifetime) of the PNB starting from 60 to 70 ns (Fig. 2d). Below this threshold size PNBs did not induce significant death among any cells and thus were considered as non-invasive. Larger PNBs (with a lifetime of 200 ns and above) killed cancer cells mechanically (non-thermally) through their immediate disruption (the mechanism of cell destruction with PNBs alone was studied in detail earlier [26,27]). In the current study we applied much smaller PNBs (20–90 ns, that alone showed little toxicity) to the cells (Fig. 2d) with mixed NS-Doxil clusters. 72 h after the PNB treatment, we observed a significant (up to 31 time) increase in the level of cancer cell death for low doses of Doxil (about 20-fold reduced, Fig. 2c) and for small (otherwise non-invasive) PNBs (with the lifetimes 30–50 ns, Fig. 2d). Normal cells, by contrast, retained high viability (Fig. 2b, Table 1) since they generated almost no or very small PNBs and took lower loads of Doxil liposomes that were not disrupted by PNBs and thus did not cause much toxicity. Furthermore, as can be seen in Fig. 2b, even bystander normal cells were not killed. Therefore, small PNBs co-localized with clustered Doxil synergistically and selectively enhanced the efficacy of chemotherapy (compared to the efficacy of PNBs and Doxil applied alone, see Fig. 2c,d) to the level sufficient to selectively kill drug-resistant cancer cells while sparing bystander normal cells. The synergistic nature of this mechanism, PNBEE, is associated with the intracellular and localized release of the drug (compared to the action of the extracellular drug or of slowly leaking intact liposomes). We next explored the mechanism of PNBEE chemotherapy in detail in several experiments as outlined below.

3.2. PNBEE mechanism

To understand the role of the cell-assembled mixed NS-Doxil nanoclusters and the mechanism of the suggested method, we compared the therapeutic effect of the two extracellular and similar drugs, a free solution of Doxorubicin and stock non-conjugated Doxil liposomes to the above studied Doxil-Panitumumab conjugates. Several different combinations of drug and PNB treatment were applied using Doxil-Panitumumab conjugates (Fig. 3a), stock unconjugated Doxil (Fig. 3b) and Doxorubicin solution (Fig. 3c): drug alone, NSs alone, NSs and drug, PNBs alone, PNBs in presence of the extracellular drug and PNBs with the extracellular drug removed prior to the PNB treatment. First of all, we discovered that PNBs increased the therapeutic efficacy of even free extracellular Doxorubicin at relatively low concentration of 5 μg/ml (Fig. 3c) and of passively targeted (also extracellular) Doxil at the concentration of 20 μg/ml (Fig. 3b), providing that the PNBs were generated in presence of the extracellular drugs. However, the removal of both drugs prior to the PNB treatment (identically to the experiments with Doxil conjugates described above and shown in Fig. 2) returned no therapeutic effect at all, contrary to that of Doxil conjugates (red bars in Fig. 3). This experiment proved that the internalization of Doxil liposomes and their co-localization with PNBs are critical for the PNBEE mechanism because neither Doxorubicin or Doxil were internalized by cancer cells in this experiment and remained extracellular. Observed therapeutic effect of extracellular drugs cannot be

attributed to PNBEE and involves different mechanism, such as PNB-induced permeation of cellular membrane and injection of the extracellular drug. The latter mechanism is the subject of a separate study and was demonstrated in our previous work [28]. Achieving a comparable therapeutic effect with extracellular drugs required larger PNBs and respectively higher laser fluences, increased drug doses, increased from 24 h to 72 h times of exposure to drugs, and resulted in higher non-specific toxicity compared to the PNBEE mechanism (Table 1). In the case of Doxil, the leakage of Doxorubicin through the intact liposome membrane is believed to cause the therapeutic (and nonspecific) effect [42].

On the contrary, in the PNBEE method (Table 1), the exposure to the drug was reduced to the time required for initial targeting (24 h in our experiments, although this time could be reduced even to 1 h that would still provide the endocytotic formation of the mixed clusters [29]), the drug dose was maximally reduced 20-fold from 100 μg/ml to 5 μg/ml, minimal PNBs (and minimal optical energy) were required and the minimal non-specific toxicity was achieved. This is the important difference between PNBEE chemotherapy and other chemotherapeutic methods: PNBEE employs only the drug accumulated in the intracellular nanoclusters and does not require any extracellular drug at the time of activation of the therapy with a laser pulse. This tremendously reduces the non-specific toxicity of PNBEE chemotherapy while the intracellular release of the encapsulated drug overcomes the drug resistance of the cells and bypasses numerous biological barriers. Based on the results obtained for NS and Doxil targeting, PNB generation and associated cell death levels in target and normal cells we suggest the following mechanism for PNBEE drug delivery:

1. A PNB is selectively generated only around the largest endosomal clusters of NS-drug at the minimal level of laser fluence, i.e. only in the target cell.
2. The co-localization of the PNB with drug liposomes and cellular endosomes provides their mechanical disruption by the expanding PNB and the fast release (ejection) of the drug into the cytoplasm within nanoseconds. (The effect of PNB-induced disruption of liposomes and of the release of their fluorescent molecular cargo was demonstrated earlier by us for free individual liposomes in water [30]).
3. A single PNBEE event (induced with a single short laser pulse) is sufficient for the therapeutic effect.

The two key components of the PNBEE mechanism are a cancer cell self-assembled mixed NP-drug nanocluster and co-localized on-demand generation of small PNBs. Separate targeting of the two components (gold NPs and drug or other molecular cargo) provides better selectivity compared to administering complex NPs with all components (gold NPs and the drug) pre-loaded into the same complex particle [8,9,12,43], due to the unavoidable nonspecific accumulation of such particles in normal cells and their reduced internalization due to their increased size.

In all the experiments described above, despite quite different conditions, we observed similar correlations between the parameters of optically detected PNB signals (the lifetime) and the efficacy of the chemotherapeutic effect (Fig. 2d). Since PNBs were simultaneously detected in individual cells, we can use the optical signal of PNB for the real-time and cell-level guidance of the drug release. On the other hand the PNB lifetime is determined by the energy (fluence) of the excitation laser pulse (Fig. 1i). Therefore, by monitoring PNB signals we can dynamically control the laser pulse fluence to tune and maintain the size of the PNB to specific margins that provide an optimal chemotherapeutic effect. In addition, PNB signals can be used for detecting target cells [26–29]. Besides monitoring the optical scattering signal of the PNB, its acoustical emission can be also detected with an ultrasound transducer in a way similar to opto-acoustic imaging systems. All PNB -related signals are very short, within 10^{-7-8} s and can be used for adjusting the fluence of the laser pulses in

real-time with commercially available high-speed optical attenuators. Therefore, in addition to their therapeutic function, PNBs provide real-time guidance and that can be used for dynamic optimization of the PNB size, the main parameter that determines the therapeutic efficacy. Due to dynamic tunability of plasmonic nanobubbles (Fig. 1i) the PNBEE method can be seamlessly integrated with another PNB-based treatments by increasing the maximal diameter of the PNB for mechanical ablation of target cells and tissues [26,27]. Therefore this technology can potentially provide an efficient combination of guided chemotherapy and micro-surgery.

4. Conclusions

To summarize, PNBEE (plasmonic nanobubble-enhanced endosomal escape) mechanism demonstrated the potential for intracellular drug delivery into specific individual target cells during the guided and fast treatment of heterogeneous cell systems:

1. Active drug was delivered and released in specific target cells within a nanosecond through the co-localization of the encapsulated drug and gold NPs in the self-assembled by the cancer cells mixed nanoclusters and their on-demand mechanical disruption and drug ejection by co-localized plasmonic nanobubbles.
2. A synergistic and selective intracellular effect of the plasmonic nanobubbles and the drug results in 31-fold enhancement of chemotherapeutic efficacy of standard drug (Doxil) and thus overcomes drug resistance of cancer cells, and in 10-fold reduction of its non-specific toxicity, 20-fold reduction of the drug dose and 3-fold reduction of the drug administration time thus sparing bystander normal cell even though they are heterogeneously mixed with target cells.

Acknowledgments

Authors thank Drs. Joseph Zasadzinski of the University of Minnesota and Dr. Gary Braun of the University of California Santa Barbara for their help with the fabrication of hollowgold nanoshells, Dr. Xiaoyang Ren of the UT MDAnderson Cancer Center for his help with cell culturing and Dr. Daniel Wagner of Rice University for valuable discussions of the method. Ms. Sue Parminter kindly copyedited this manuscript. This work was supported in part by National Institute of Health Grant R01GM094816. Confocal microscopy was performed on equipment obtained through a Shared Instrumentation Grant from the National Institutes of Health (S10RR026399-01).

References

1. Cho K, Wang X, Nie S, Chen ZG, Shin DM. Therapeutic nanoparticles for drug delivery in cancer. Clin Cancer Res. 2008; 14:1310–1316. [PubMed: 18316549]
2. Peer D, Karp JM, Hong S, Farokhzad OC, Margalit R, Langer R. Nanocarriers as an emerging platform for cancer therapy. Nat Nanotechnol. 2007; 2:751–760. [PubMed: 18654426]
3. Meng H, Liong M, Xia T, Li Z, Ji Z, Zink JI, et al. Engineered design of mesoporous silica nanoparticles to deliver doxorubicin and P-glycoprotein siRNA to overcome drug resistance in a cancer cell line. ACS Nano. 2010; 4:4539–4550. [PubMed: 20731437]
4. Liang XJ, Meng H, Wang Y, He H, Meng J, Lu J, et al. Metallofullerene nanoparticles circumvent tumor resistance to cisplatin by reactivating endocytosis. Proc Natl Acad Sci USA. 2010; 107:7449–7454. [PubMed: 20368438]
5. Sajja HK, East MP, Mao H, Wang YA, Nie S, Yang L. Development of multifunctional nanoparticles for targeted drug delivery and noninvasive imaging of therapeutic effect. Curr Drug Discov Technol. 2009; 6:43–51. [PubMed: 19275541]
6. Prabaharan M, Grailer JJ, Pilla S, Steeber DA, Gong SQ. Gold nanoparticles with a monolayer of doxorubicin-conjugated amphiphilic block copolymer for tumor-targeted drug delivery. Biomaterials. 2009; 30:6065–6075. [PubMed: 19674777]

7. Yuk SH, Oh KS, Koo H, Jeon H, Kim K, Kwon IC. Multi-core vesicle nanoparticles based on vesicle fusion for delivery of chemotherapic drugs. Biomaterials. 2011; 32:7924–7931. [PubMed: 21784512]
8. Wu GH, Milkhailovsky A, Khant HA, Fu C, Chiu W, Zasadzinski JA. Remotely triggered liposome release by near-infrared light absorption via hollow gold nanoshells. J Am Chem Soc. 2008; 130:8175–8177. [PubMed: 18543914]
9. Braun GB, Pallaoro A, Wu G, Missirlis D, Zasadzinski JA, Tirrell M, et al. Laser-activated gene silencing via gold nanoshell-siRNA conjugates. ACS Nano. 2009; 3:2007–2015. [PubMed: 19527019]
10. Wang F, Wang YC, Dou S, Xiong MH, Sun TM, Wang J. Doxorubicin-tethered responsive gold nanoparticles facilitate intracellular drug delivery for overcoming multidrug resistance in cancer cells. ACS Nano. 2011; 5:3679–3692. [PubMed: 21462992]
11. Kim B, Han G, Toley BJ, Kim CK, Rotello VM, Forbes NS. Tuning payload delivery in tumour cylindroids using gold nanoparticles. Nat Nanotechnol. 2010; 5:465–472. [PubMed: 20383126]
12. Paasonen L, Sipila T, Subrizi A, Laurinmaki P, Butcher SJ, Rappolt M, et al. Gold-embedded photosensitive liposomes for drug delivery: triggering mechanism and intracellular release. J Control Release. 2010; 147:136–143. [PubMed: 20624434]
13. Pissuwan D, Niidome T, Cortie MB. The forthcoming applications of gold nanoparticles in drug and gene delivery systems. J Control Release. 2011; 149:65–71. [PubMed: 20004222]
14. Musacchio T, Torchilin VP. Recent developments in lipid-based pharmaceutical nanocarriers. Front Biosci. 2011; 16:1388–1412. [PubMed: 21196238]
15. Kuykendall DW, Zimmerman SC. Nanoparticles - A very versatile nanocapsule. Nat Nanotechnol. 2007; 2:201–202. [PubMed: 18654259]
16. Fechheimer M, Boylan JF, Parker S, Sisken JE, Patel GL, Zimmer SG. Transfection of mammalian cells with plasmid DNA by scrape loading and sonication loading. Proc Natl Acad Sci USA. 1987; 84:8463–8467. [PubMed: 2446324]
17. Prentice P, Cuschierp A, Dholakia K, Prausnitz M, Campbell P. Membrane disruption by optically controlled microbubble cavitation. Nat Phys. 2005; 1:107–110.
18. Yoshida S, Kashiwamura SI, Hosoya Y, Luo E, Matsuoka H, Ishii A, et al. Direct immunization of malaria DNA vaccine into the liver by gene gun protects against lethal challenge of Plasmodium berghei sporozoite. Biochem Biophys Res Commun. 2000; 271:107–115. [PubMed: 10777689]
19. Lee S, McAuliffe DJ, Flotte TJ, Kollias N, Doukas AG. Photomechanical transcutaneous delivery of macromolecules. J Invest Dermatol. 1998; 111:925–929. [PubMed: 9856797]
20. Qiu Y, Luo Y, Zhang Y, Cui W, Zhang D, Wu J, et al. The correlation between acoustic cavitation and sonoporation involved in ultrasound-mediated DNA transfection with polyethylenimine (PEI) in vitro. J Control Release. 2010; 145:40–48. [PubMed: 20398711]
21. Haas K, Sin WC, Javaherian A, Li Z, Cline HT. Single-cell electroporation for gene transfer in vivo. Neuron. 2001; 29:583–591. [PubMed: 11301019]
22. Soughayer JS, Krasieva T, Jacobson SC, Ramsey JM, Tromberg BJ, Allbritton NL. Characterization of cellular optoporation with distance. Anal Chem. 2000; 72:1342–1347. [PubMed: 10740880]
23. Stevenson D, Agate B, Tsampoula X, Fischer P, Brown CTA, Sibbett W, et al. Femtosecond optical transfection of cells: viability and efficiency. Opt Express. 2006; 14:7125–7133. [PubMed: 19529083]
24. Lukianova-Hleb E, Hu Y, Latterini L, Tarpani L, Lee S, Drezek RA, et al. Plasmonic nanobubbles as transient vapor nanobubbles generated around plasmonic nanoparticles. ACS Nano. 2010; 4:2109–2123. [PubMed: 20307085]
25. Lukianova-Hleb E, Lapotko DO. Influence of transient environmental photothermal effects on optical scattering by gold nanoparticles. Nano Lett. 2009; 9:2160–2166. [PubMed: 19374436]
26. Wagner DS, Delk NA, Lukianova-Hleb EY, Hafner JH, Farach-Carson MC, Lapotko DO. The in vivo performance of plasmonic nanobubbles as cell theranostic agents in zebrafish hosting prostate cancer xenografts. Biomaterials. 2010; 31:7567–7574. [PubMed: 20630586]
27. Lukianova-Hleb E, Hanna EY, Hafner JH, Lapotko DO. Tunable plasmonic nanobubbles for cell theranostics. Nanotechnology. 2010; 21:82102.

28. Lukianova-Hleb E, Samaniego A, Wen J, Metelitsa L, Chang C-C, Lapotko D. Selective gene transfection of individual cells in vitro with plasmonic nanobubbles. J Control Release. 2011; 152:286–293. [PubMed: 21315120]
29. Lapotko DO, Lukianova-Hleb EY, Oraevsky AA. Clusterization of nanoparticles during their interaction with living cells. Nanomedicine (Lond). 2007; 2:241–253. [PubMed: 17716124]
30. Anderson L, Hansen E, Lukianova-Hleb EY, Hafner JH, Lapotko DO. Optically guided controlled release from liposomes with tunable plasmonic nanobubbles. J Control Release. 2010; 144:151–158. [PubMed: 20156498]
31. Wu G, Mikhailovsky A, Khant HA, Zasadzinski JA. Chapter 14-Synthesis, characterization, and optical response of gold nanoshells used to trigger release from liposomes. Methods Enzymol. 2009; 464:279–307. [PubMed: 19903560]
32. Laser Institute of America. American national standard for safe use of lasers. 2000 (ANSI Z136.1–2000).
33. Park JW, Mamot C, Drummond DC, Greiser U, Hong K, Kirpotin DB, et al. Epidermal growth factor receptor (EGFR)-targeted immunoliposomes mediate specific and efficient drug delivery to EGFR- and EGFRvIII-overexpressing tumor cells. Cancer Res. 2003; 63:3154–3161. [PubMed: 12810643]
34. Lukyanov AN, Elbayoumi TA, Chakilam AR, Torchilin VP. Tumor-targeted liposomes: doxorubicin-loaded long-circulating liposomes modified with anti-cancer antibody. J Control Release. 2004; 100:135–144. [PubMed: 15491817]
35. Elbayoumi TA, Torchilin VP. Enhanced cytotoxicity of monoclonal anticancer antibody 2C5-modified doxorubicin-loaded PEGylated liposomes against various tumor cell lines. Eur J Pharm Sci. 2007; 32:159–168. [PubMed: 17707615]
36. Hleb E, Hafner JH, Myers JN, Hanna EY, Rostro BC, Zhdanok SA, et al. LANTCET: elimination of solid tumor cells with photothermal bubbles generated around clusters of gold nanoparticles. Nanomedicine (Lond). 2008; 3:647–667. [PubMed: 18817468]
37. Chithrani BDCW. Elucidating the mechanism of cellular uptake and removal of protein-coated gold nanoparticles of different sizes and shapes. Nano Lett. 2007; 2007(7):1542–1550.
38. Salmaso S, Caliceti P, Amendola V, Meneghetti M, Magnusson JP, Pasparakis G, et al. Cell uptake control of gold nanoparticles functionalized with a thermoresponsive polymer. J Mater Chem. 2009; 19:1608–1615.
39. Neumann J, Brinkmann R. Nucleation dynamics around single microabsorbers in water heated by nanosecond laser irradiation. J Appl Phys. 2007; 101 114701.
40. Vanleeuwen TG, Jansen ED, Motamedi M, Welch AJ, Borst C. Excimer-laser ablation of soft-tissue - a study of the content of rapidly expanding and collapsing bubbles. IEEE J Quantum Elect. 1994; 30:1339–1347.
41. Vogel A, Noack J, Huttman G, Paltauf G. Mechanisms of femtosecond laser nanosurgery of cells and tissues. Appl Phys B-Lasers O. 2005; 81:1015–1047.
42. Doxil. Product information book. Vol. vol. 3. L.P USA: Centocor Ortho Biotech Products; 2011.
43. Qin G, Li Z, Xia R, Li F, O'Neill BE, Goodwin JT, et al. Partially polymerized liposomes: stable against leakage yet capable of instantaneous release for remote controlled drug delivery. Nanotechnology. 2011; 22 155605.

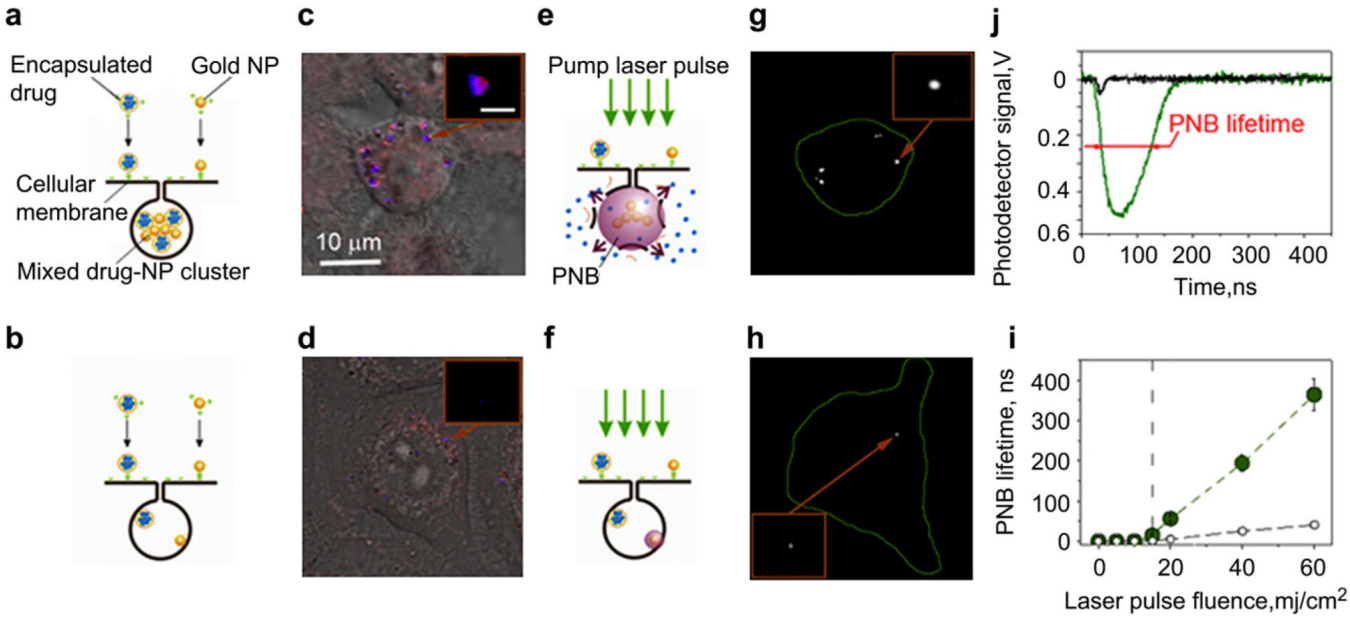

Fig. 1.

Targeting of cancer (top panel) and normal (bottom panel) cells with NS, Doxil drug (Doxorubicin in liposomes) and PNBs. a, b, Principle of separate administration of gold NPs and encapsulated drugs and of receptor-mediated endocytosis-driven self-assembly by cancer cell a of the mixed NP-drug nanocluster, that does not emerge in normal cell b. c, d, confocal images of cancer c and normal d cells show NSs (blue, optical scattering mode) and Doxil (red, fluorescence mode) co-localized clusters (insert) only for cancer cells (scale bar is 400 nm insert) and no clusters for normal cells d. e, f, Selective generation of PNB around large NS-Doxil cluster disrupts liposome, endosome and ejects the drug into the cytoplasm in cancer cell e while the lack of PNB and of its co-localization with Doxil in normal cell f does not release even non-specifically taken drug. g, h, Time-resolved optical scattering images of PNBs show their co-localization with NS-Doxil nanoclusters in cancer cell g, and much smaller PNB in normal cell h. j, optical time-responses obtained from cancer (green) and normal (black) cells were used to measure the PNB size through their lifetime. i, Dependence of the PNB lifetime in cancer (green solid dots) and normal (black hollow dots) cells upon laser pulse fluence shows tunable and selective generation of PNBs. (For interpretation of the references to colour in this figure legend, the reader is referred to the web version of this article.)

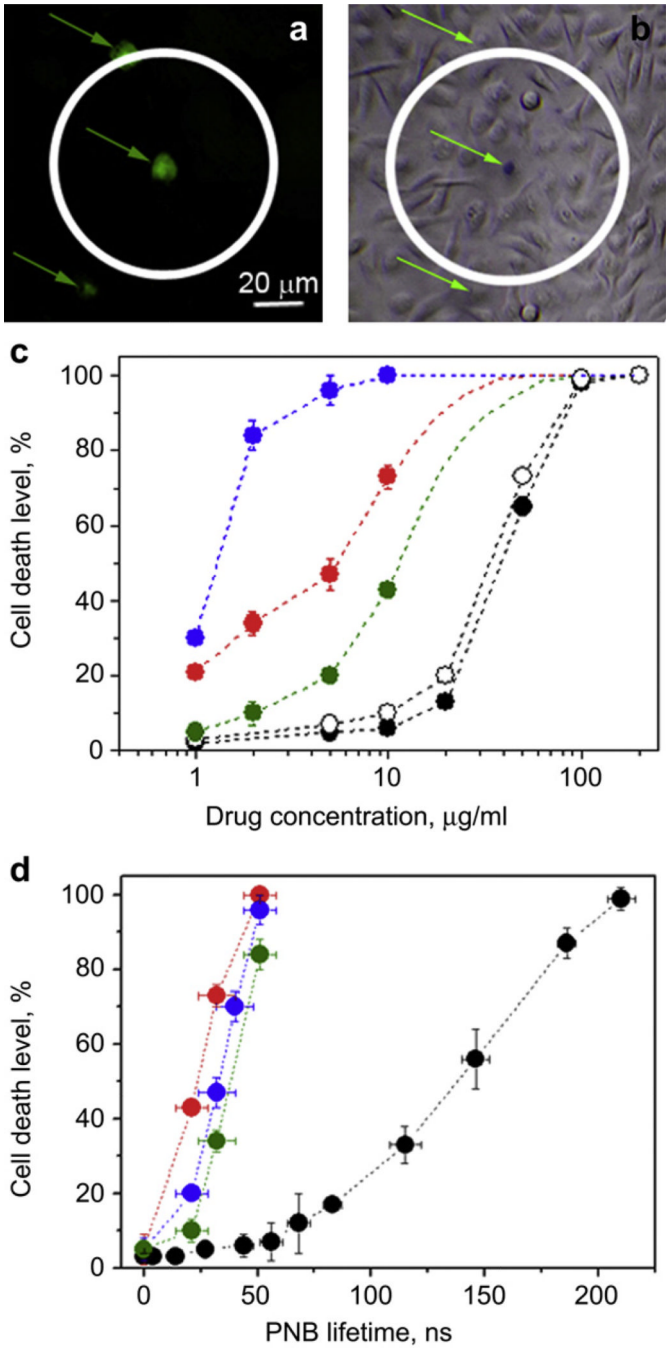

Fig. 2.

The therapeutic effect of Doxil, plasmonic nanobubbles and PNBEE mechanism in a co-culture of cancer (HN31, solid dots) and normal (NOM9, hollow dots) cells. a, Fluorescent image identifies cancer cells though green fluorescence (indicated with green arrows) before PNBEE treatment (white circle shows laser beam). b, Bright field image of the same area as in a obtained 72 h after the PNBEE treatment shows dead (blue) and live (colorless) cells. Cell death level among cancer and normal cells as function of the concentration of Doxil-Panitumumab conjugate, c, measured 72 h after the PNBEE treatment at the different size (lifetime) of PNBs: black - 0 (no PNB), green - 21 ± 7 ns, red - 32 ± 8 ns, blue - 51 ± 7 ns. d, Cancer cell death level as function of the PNB size (lifetime) as measured 72 h after PNBEE

treatment under the different concentrations of Doxil-Panitumumab conjugates (μg/ml): black - 0 (no drug), green - 2, blue - 5, red - 10. In all cases the extracellular drug was removed before generating the PNBs. (For interpretation of the references to colour in this figure legend, the reader is referred to the web version of this article.)

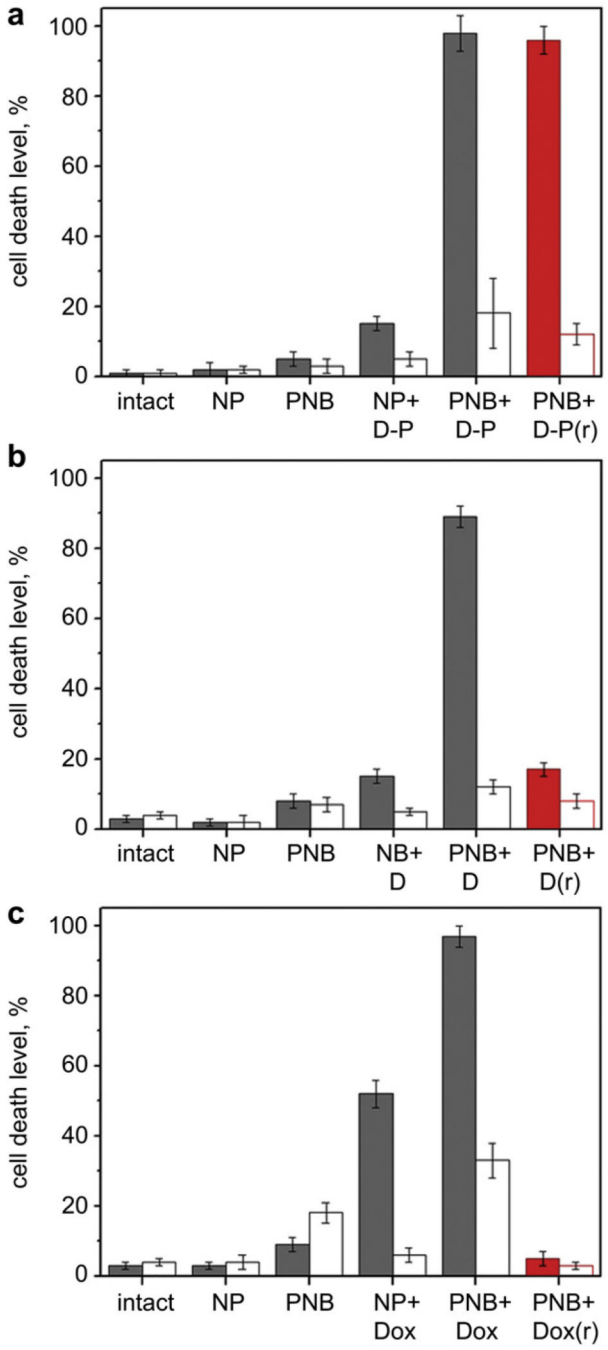

Fig. 3.

The cell death level among cancer (grey and red) and normal (white) cells measured 72 h after the following treatments: intact cells (no treatment), NPs alone, NPs with drug (NP + D or Dox), PNBs alone, PNBs in presence of extracellular drug (PNB + D or + Dox), PNBs applied after removal of the extracellular drug (PNB+D-P(r) or PNB+D(r) or PNB+Dox(r), red). a, PNBEE method (Doxil-Panitumumab(D–P) conjugates at 5 μg/ml @ 24 h incubation). b, Injection of extracellular stock Doxil (D) (20 μg/ml @ 72 h incubation). c, Injection of the extracellular free Doxorubicin (Dox) (5 μg/ml @ 72 h incubation). Red bars correspond to the PNBEE mode. (For interpretation of the references to colour in this figure legend, the reader is referred to the web version of this article.)

Table 1

Experimental and therapeutic parameters for PNBEE and for delivery of extracellular drugs.

Mechanism of drug delivery		**PNBEE**		**Delivery of extracellular drug**			
Drug		Doxil-Panitumumab conjugate		Stock Doxil (encapsulated Doxorubicin)		Doxorubicin (free solution)	
Drug dose (concentration @ incubation time), μg/ml@h		5 @ 24		20 @ 72		5 @ 72	
Laser pulse fluence (820 nm, 70 ps), mJ/cm^2		15	0	20	0	25	0
PNB size (lifetime), ns	Target cells	51 ± 7	–	65 ± 8	–	90 ± 10	–
	Non-specific cells	4 ± 2		11 ± 4		9 ± 5	
Cell death level, %	Target cells	96 ± 2	5 ± 2	98 ± 2	8 ± 2	97 ± 2	9 ± 2
	Non-specific cells	12 ± 3	7 ± 2	15 ± 2	11 ± 2	33 ± 5	18 ± 3